International Journal of Grid and High Performance Computing
Volume 15 • Issue 2

Duck Pack Optimization With Deep Transfer Learning-Enabled Oral Squamous Cell Carcinoma Classification on Histopathological Images

Savita K. Shetty, Department of Computer Science and Engineering, Ramaiah Institute of Technology, Bangalore, India & Visvesvaraya Technological University, Belagavi, India*

https://orcid.org/0000-0003-1046-5138

Annapurna P. Patil, Department of Computer Science and Engineering, Ramaiah Institute of Technology, Bangalore, India & Visvesvaraya Technological University, Belagavi, India

https://orcid.org/0000-0003-4604-428X

ABSTRACT

Earlier detection and classification of squamous cell carcinoma (OSCC) is a widespread issue for efficient treatment, enhancing survival rate, and reducing the death rate. Thus, it becomes necessary to design effective diagnosis models for assisting pathologists in the OSCC examination process. In recent times, deep learning (DL) models have exhibited considerable improvement in the design of effective computer-aided diagnosis models for OSCC using histopathological images. In this view, this paper develops a novel duck pack optimization with deep transfer learning enabled oral squamous cell carcinoma classification (DPODTL-OSC3) model using histopathological images. The goal of the DPODTL-OSC3 model is to improve the classifier outcomes of OSCC using histopathological images into normal and cancerous class labels. Finally, the variational autoencoder (VAE) model is utilized for the detection and classification of OSCC. The performance validation and comparative result analysis for the DPODTL-OSC3 model are tested using a histopathological imaging database.

KEYWORDS

Computer Vision, Computer-Aided Diagnosis, Deep Learning, Duck Pack Optimization, Image Classification, Oral Cancer, Parameter Optimization

1. INTRODUCTION

Oral cancer, which is one of the most common and deadly diseases in the world, has been a significant issue for the general public's health for a good number of years. It is estimated that 475,000 new instances of the subtype of head and neck cancer known as oral cancer will be discovered each year. It is estimated that approximately 80% of patients will survive the disease's early stages, while only

DOI: 10.4018/IJGHPC.320474 *Corresponding Author

20% will survive the disease's later stages (Amin, I., 2021 and Chu, C. S., 2021). Squamous cell carcinoma of the oral cavity is responsible for the majority of cases of oral cancer, which accounts for around 85 percent of all cases. Even though primary detection of oral cancer is vital, the majority of patients are diagnosed with the disease after it has progressed, leaving them with a poor prognosis. This is because early detection of oral cancer is essential. despite the fact that oral cancer screenings at an early stage are crucial. This is the situation, despite the fact that discovering oral cancer in its early stages is extremely important. The clinical appearance of oral cancer does not adequately represent the dysplastic condition, analysis, or severity of the illness; hence, therapeutic suggestions that are based solely on the clinical appearance are insufficient. Oral cancer has many risk factors and a low post-treatment survival rate (Arun, A. 2021 and Das, D. K., 2018). Biological and medical models of connected and lesion-free tumours can be detected in various body locations without stereotypes and appearance models. High-risk patients have leukoplakia, erythroplasia, and oral submucosal fibrosis. Malignant and benign tumours must be differentiated. Age, gender, and smoking affect oral cancer prognosis (Jain, M., 2014). AI can tackle every healthcare problem (Cyril, C. P. D., 2021). Unhealed sores or ulcers that are painful or bleeding often indicate malignancy. Symptoms of oral cancer include non-healing white or red lesions on the lips, gums, tongue, or mouth; a lump or tumour in the mouth; loose teeth; trouble speaking or swallowing; a swollen jaw; and chronic throat pain. Oral cancer can also spread to other parts of the body.

The most common type of cancer of the lips and oral cavity is oral squamous cell carcinoma (OSCC), which has a high mortality rate due to diagnostic delays brought on by early-stage misdiagnosis. The gold standards for diagnosing OSCC are histopathological analysis and biopsies, but these procedures are time-consuming, invasive, and not always acceptable to patients, especially when additional biopsies are required as part of a follow-up. The diagnostic approach is enhanced using adjunctive non-invasive imaging techniques, which also makes it more efficient and well-liked by patients. The goal of the current review is to highlight the most well-established diagnostic methods, such as tissue autofluorescence and vital staining, and to discuss the potential applications of some of the most innovative methods currently being developed, including narrow-band imaging, high-frequency ultrasounds, optical coherence tomography, and in vivo confocal microscopy. An ideal three-step diagnostic process is suggested considering their contribution to the diagnosis of OSCC to improve the speed, quality, and accuracy of the diagnostic process (Romano, A,2021).

Early detection by general dentists (GPs) is thought to improve the prognosis of oral cancer. A biopsy is the gold standard method of determining the presence of oral cancer. The procedure, however, is extremely invasive and painful. A biopsy may necessitate specialised training for general practitioners, and the dissemination of cancer cells into the circulation increases the risk of metastasis following the biopsy. Screening should be non-invasive, low-cost, and repeatable. Oral cancer screening methods include cytology, vital staining, and FV. Fluorescence visualization (FV) oral cancer detection Subjective evaluation in this study revealed high sensitivity (96.8%) but low specificity (48.4%). Because this difference in accuracy was for subjective evaluation, it was assumed that evaluators differed significantly. As a result, in this study, we used image processing analysis to perform subjective and objective evaluation (Kikuta S .,2018 and Kozakai A.,2019).

Artificial intelligence can address present problems with illness identification and prognosis prediction when employed to treat oral malignant growths. Scientists from all over the world are interested in artificial intelligence, a technology advancement that mimics human cognitive abilities (Panigrahi, S. 2020). It has just lately been used to dentistry, but the outcomes are astonishing. Beginning in the year 300 B.C. C. A well-known model of brain operation was developed by Plato. The artificial intelligence system is a framework that takes in data, recognises designs, learns from data, and generates results (Sunitha, G. 2022). Training and testing are the two phases of artificial intelligence operation. The training data determines the model set's parameters. The model uses information from past events, such as patient information or information from other cases, to create predictions in hindsight. The testing phase follows with the application of these criteria. Multiple studies have

identified oral cancer prognostic indications based on biomarkers discovered by artificial intelligence. The sooner a malignant tumour is discovered, the greater the patient's probability of survival and the number of possible treatments (Mishra, S. 2022, Rahman, T. Y. 2018 and Saravanakumar, C., 2022).

In recent years, deep learning techniques have attracted considerable interest due to their potential applications and purported benefits in cancer prediction. This is meant to promote and encourage better patient health management by assisting doctors in making more informed decisions on patient health. Surprisingly, technical progress has facilitated the shift from neural networks to deep neural networks. Attention has also been drawn to this technology's capacity to improve cancer management.

Patients with oral cancer who are diagnosed and treated early have a greater probability of survival. Only by utilising a system that combines machine learning with deep learning is it possible to accurately forecast the complex and rapidly growing disease known as mouth cancer. The researchers employed machine learning methods to forecast verbal tumor in its initial phases. Investigators have developed several histopathological machine learning algorithms that can be utilised to combat tumor. Using present information and a range of neural algorithms, a research team has created a way for accurately identifying cancer based on machine learning. In the past, cloud-based deep learning algorithms were utilised to enhance cancer patient therapy and reduce their high fatality rate. Deep learning approaches paired with machine learning technology facilitate the linking of genes in the battle against cancer. Researchers successfully predicted cancer from digital images using deep CNN and artificial neural networks.

Panigrahi et al. Proposed a capsule network model based on deep learning to classify malignant tumors in the oral cavity. The capsule mesh was applied in agreement with consensual and dynamic routing to make it more robust for afferent rotation and affine transformation to analyse histopathological images of OSCC with high accuracy. Histopathology is crucial in the diagnosis of diseases. To pinpoint the precise location of diseased cells, biological tissues must be examined. Typically, a biopsy is required. The best test to date for detecting cancer is a biopsy. Under a microscope, the biopsy slides are examined according to various cytological standards. Consequently, there is a high likelihood that results won't be reproducible and uniform. Using a common data set of histopathology pictures generated by biopsy and evaluated by two pathologists. A pathologist's histopathological tissue analysis is the only conclusive method for (a) confirming the presence or absence of disease and (b) disease grading or measuring disease progression. A single core of prostate biopsy tissue digitised at 40x resolution contains about 15,000 15,000 elements, or about 225 million pixels. In this context, a single prostate biopsy procedure can generate 12 to 20 biopsy samples, or 2.5 to 4 billion pixels of data per patient study. These images are frequently processed in a multiresolution framework due to their relatively large size and content.

Rahman et al. (2022) describes a two-stage AI-based method for identifying oral squamous cell cancer. These must be addressed in classification algorithms. Textural features of images were extracted and used to categorise the images into normal and malignant categories using Histogram and grey-level co-occurrence matrix approaches. This method yielded 100% classification accuracy. These images can also be used to perform cellular or nuclear analysis. One such nuclear analysis has already been carried out. Changes in the nucleus, such as size, shape, and so on, play a critical role in distinguishing a normal cell from a malignant one. The repository is composed of 1224 images divided into two sets of images with two different resolutions by Rahman, T. Y. 2017. First set consists of 89 histopathological images with the normal epithelium of the oral cavity and 439 images of Oral Squamous Cell Carcinoma (OSCC) in 100x magnification. The second set consists of 201 images with the normal epithelium of the oral cavity and 495 histopathological images of OSCC in 400x magnification. The images were captured using a Leica ICC50 HD microscope from Hematoxyline and Eosin (H&E) stained tissue slides collected, prepared, and catalogued by medical experts from 230 patients. A subset of 269 images from the second data set was used to detect OSCC based on textural features.

Fraz et al. (2022) However, most publicly available data is made up of Hematoxylin and Eosin (H&E)-stained pathology images, for which immunohistochemistry images are difficult to obtain.

Because of their complexity and heterogeneity, the role of microvessels in H&E-stained images has received little attention. To assess intratumoral heterogeneity, it is necessary to collect information on the precise distribution of a tumour. The gold standard for diagnosing tumours is hematoxylin and eosin staining, which has been used by pathologists for more than a century. However, it is difficult to acquire the three-dimensional distribution of cells in solid tumours after staining and rinsing entire tumour tissues with H&E . In this paper, we propose a modified method for H&E staining in which delipidation and ultrasound waves are used to increase tissue permeability and accelerate dye diffusion. This enhanced hematoxylin and eosin staining technique is known as iHE (intact tissue H&E staining). Mice with intact organs were stained with the iHE method, sectioned, and imaged sequentially. The results demonstrated that the entire tissue was stained uniformly. Combined with micro-optical sectioning tomography (MOST), the iHE method enables 3D volume imaging and spatial evaluation of the intratumoral heterogeneity of the entire tumour tissue.

Early detection and treatment of oral cancer can improve a patient's chances of surviving the disease, according to research published by A. Alhazmi et al. Due to its complexity, C.S. Mouth cancer, according to Chu et al, Therefore, the researchers are responsible for providing the necessary merging apparatus. R.A. Welikala and coworkers Researchers can choose from a variety of histopathological machine learning algorithms to aid with the ongoing war against cancer. Researchers have come up with a unified machine learning-based strategy for making in-the-moment cancer predictions. They used several neural algorithms, and their forecasts ended up being good.

An effective strategy for categorising and identifying oral tumours is provided by Bhandari et al. in their study. To reduce the number of inaccurate oral cancer classifications and prognoses, the technique under consideration employs a convolution neural network with an enhanced damage purpose. A technique for automatically identifying oral tumours on cytology slides was developed by Lu et al. Included in the method are convolution regression nucleus identification, per-cell focus selection, and CNN-based classification. The pipeline includes fully convolutional regression-based nucleus recognition, per-cell focus selection, and CNN-based classification. Faster per-cell focus decisions with human-level accuracy are provided by the suggested approach. Computer-aided systems are essential for accurately automatically separating benign from malignant OSCC cells based on the characteristics of each tumour. Additionally, utilising artificial intelligence techniques to enhance diagnosis is promising, particularly machine learning and deep learning. Deep learning techniques have shown they can accurately diagnose and analyse biomedical images, despite taking a lot of time. One of the most effective deep learning techniques for this is to use conventional neural network (CNN) models. The CNN models are initially trained to know the features of each disease by comparing the features of each new image (test) with the features in the stored (training data). The CNN model will be able to predict the unknown cases after training. However, several factors, including data set noise, a lack of data sets, unbalanced data sets, the number of layers employed, activation function, and others, affect the accuracy of CNN models. The purpose of this study was to investigate these issues that CNN models face and attempt to resolve them to achieve superior outcomes in histology diagnosis, which is essential for the early diagnosis of OSCC.

Alabi R.O et al (2021) the study wanted to see if there were any unique automation approaches that might be used to detect oral squamous cell carcinoma on clear photos. To do this, they planned to use methods like convolutional neural networks and in-depth training. This particular Convolutional Neural Network was developed to locate quotations and images, as well as to train and assess. The symptoms of oral cancer can present themselves in a wide variety of different ways and behaviours. In recent years, researchers have utilised a range of machine learning strategies to conquer cancer, and the machine learning models can identify cancer. One of these techniques is deep reinforcement learning (DNN). When it comes to the accurate prediction of oral cancer, machine learning trumps other methods. Alkhadar.H et al (2021) and Pokle, S. B., (2019) introduced the genome and a variety of pathogenic changes are the key contributors to the development of oral cancer, which is a disease with a 100% mortality rate. Patients with oral cancer who receive therapy and diagnosis at an earlier

stage have a better chance of living longer. The only way to accurately anticipate oral cancer, which is a disease that is both complex and progressing, is to use a mix of machine learning and deep learning algorithms. As a consequence of their findings, the researchers propose a collection of machine learning algorithms for the early-stage prediction of oral cancer. In their fight against cancer, researchers might employ a variety of histopathological machine learning strategies.

Using a variety of neural algorithms and real-time data, Ahmed.U et al. (2022) provide a fused machine learning-based solution for predicting cancer with high accuracy. The method is based on machine learning. In previous studies, cloud-based deep learning methods were utilised to combat malignant diseases, improve treatment, and bring down the mortality rate of females. Approaches based on machine learning can be helpful in the fight against malignant cells by assisting in the connection of genes. Researchers were able to accurately predict cancer utilising digital pictures, artificial neural networks, and deep CNN techniques. Researchers from a variety of institutions using machine learning methods to diagnose cancer in COVID patients during the COVID phase. Histopathology has been digitised is now amenable to computerised image analysis and machine learning techniques. Typically, histopathology image analysis has directly followed cytology image analysis techniques. Specifically, certain nucleus characteristics are diagnostic of cancerous conditions. Consequently, quantitative metrics for cancerous nuclei were developed and validated using cytology images to encompass the general observations of an experienced pathologist. These researchers produce extremely accurate results by employing a variety of pre-processing strategies. Deep learning radionics-based detections on cancer patients give high-quality findings when paired with other cancer treatments like chemoradiotherapy.

The Duck Pack Optimization with Deep Transfer Learning Enabled Oral Squamous Cell Carcinoma Classification (DPODTL-OSC3) prototypical was assessed on clean pictures following extensive data training and histological examination. Deep Transfer Learning mostly focuses on citation and picture searching as well as training, data, and classification. Foreseeing whether OPL patients will develop oral cancer required the use of machine learning methods and genetic information, which the researchers gathered. In this study, we present an efficient model for classifying oral squamous cell carcinomas from histopathological images using Duck Pack Optimization with Deep Transfer Learning (DPODTL-OSC3). To improve the classifier's outcome of OSCC into normal and malignant class labels is the primary goal of the DPODTL-OSC3 model. Noise in the DPODTL-OSC3 model is first removed using a Weiner filtering (WF) based preprocessing approach. In addition, the DPO technique is used for hyperparameter tuning, and a pretrained model based on EfficientNet is used for feature extraction. To further aid in OSCC detection and categorization, a variational autoencoder (VAE) model is utilized. The DPODTL-OSC3 model is evaluated by running experiments and comparing the results to a histopathology imaging database.

The following is a list of the primary contributions that this article makes:

1. In order to do a multistage classification of the OSCC, we offered three possible topologies for EfficientNet: one for well-differentiated, one for moderately differentiated, and one for poorly distinguished. These architectures function well because they offer greater accuracy and maintain information across layers.
2. The study's main objective is to train the various EfficientNet variants that have been suggested from scratch and evaluate how effective they are at solving the specified problems.
3. The proposed EfficientNet architectures offer superior performance with a small dataset by offering faster convergence and less computational complexity.
4. Data augmentation methods, activation functions, and parameter optimizations are used to avoid overfitting.

The majority of the previous studies used machine learning and deep learning approaches to forecast oral cancer using OSCC biopsies and other datasets, as shown in Table 1. However, these studies could not achieve the highest level of accuracy due to the flaws that they revealed in their

Table 1.
Analyse the strengths and flaws of prior research

References	Limitation	Dataset	Method	Accuracy
Panigrahi, S. 2020	Requires data image pre-processing techniques and Class instances	Public	Deep learning	73.87
Rahman, T. Y. 2020	Requires data pre-processing	Public	SVM	75.09
Fraz, M. M. 2020	Requires data pre-processing	Public	ANN	78.95%
Alhazmi, A. 2021	Requires data pre-processing	Public	SVM, KNN	70.59%
Welikala, R. A. 2020	Requires data pre-processing and learning criteria decision method	Public	ResNet101	78.30%
Shavlokhova, V. 2021	needs more effective methods of learning criteria and pre-processing image data	Private	CNN	77.89%
Aubreville, M. 2017	Requires data image pre-processing techniques Class instances	Public	Deep Learning	80.01%
Hardas, B. 2017	Requires handcrafted features	Public	KNN, Logistic Regression, Decision Tree, Random Forest	76%

methods. As was demonstrated in prior research, one of the primary goals of oral cancer prediction is to preserve as many lives as possible. In this article, a model that is empowered by transfer learning to predict oral cancer is proposed. The model takes information from OSCC biopsy data and trains on those features.

2. THE PROPOSED MODEL

In this article, a brand-new DPODTL-OSC3 model for the detection and categorization of oral tumours in biomedical images was presented. The DPODTL-OSC3 model initially eliminated noise content using the WF technique. The generation of higher-level deep features from the input images then makes use of the EfficientNet model. The DPODTL-OSC3 model is then used to identify and classify oral cancer. Our research has resulted in a novel approach to OSCC categorization known as DPODTL-OSC3. To test the performance of the Duck Pack Optimization with Deep Transfer Learning Enabled Oral Squamous Cell Carcinoma Classification (DPODTL-OSC3) model, a large amount of training and histology data was utilized, and noise-free images were also analyzed. The DPO algorithm's structure lends a hand in determining the best values to set its hyperparameters to. The DPODTL-OSC3 method's block diagram is shown in Figure 1.

2.1 Image Pre-Processing

The histopathology pictures are first processed using the WF method to remove any background noise. The proposed model eliminates noise by utilising Weiner filtering (WF) as a pre-processing step. In addition, the EfficientNet model is used to produce high-level, deep features from the input images. In addition, an improved Duck Pack Optimization (DPO) algorithm-based Convolutional Neural network (CNN) model is used for classifying and detecting oral cancer. It employs filtering of noisy signals through the spectral property of the desired signal and present noise, which is considered a stochastic method with linear property (Manju, B. R., 2020).

EfficientNet Rethinking Model Scaling for Convolutional Neural Networks", this paper proposes a novel model scaling technique that employs a simple yet highly effective compound coefficient to scale up CNNs in a more structured manner. Unlike conventional methods that arbitrarily scale

Figure 1.
Overall process of DPODTL-OSC3 technique

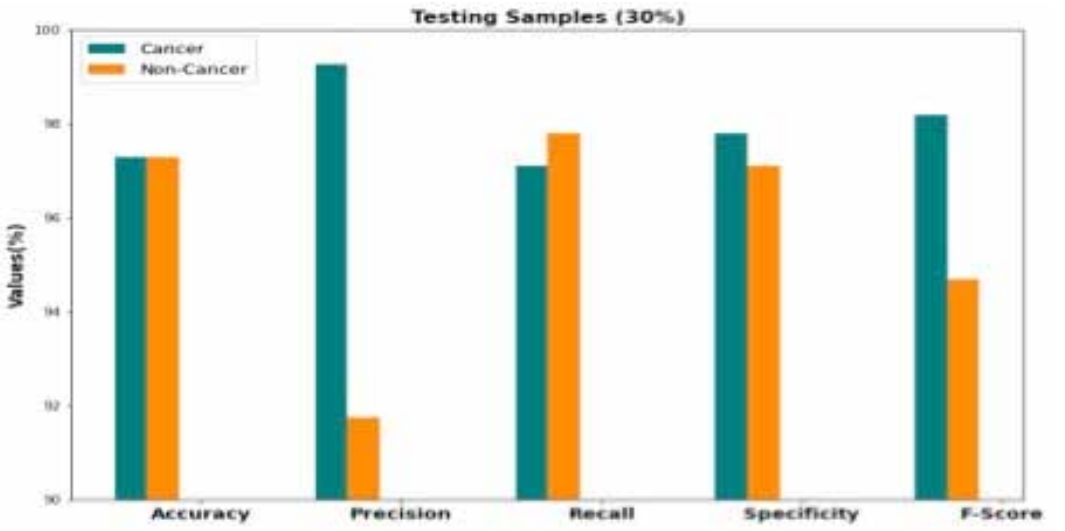

network dimensions such as width, depth, and resolution, our method scales each dimension uniformly using a fixed set of scaling coefficients. Powered by this novel scaling method and recent progress on AutoML, we've developed a family of models called EfficientNets that surpasses state-of-the-art accuracy with up to ten times greater efficiency.

(Luz et al. 2021) utilised CNN architecture to detect Covid-19 by CXR. B3-X, from the family of proposed models based on EfficientNet, has an accuracy of 93.9%, COVID-19 sensitivity of 96.8%, and 100% positivity prediction (no false negatives) while requiring 5 to 30 times fewer parameters. A dataset containing 13,569 X-ray images of healthy, COVID-19 pneumonia, and non-COVID-19 pneumonia patients was used to train the recommended approaches and the five competing architectures. A hierarchical technique and cross-dataset analysis were employed. The examination of multiple datasets revealed that even the most sophisticated models lack generalisation capability. As can be seen, this study only included a small number of images of Covid-19-positive patients. The authors evaluated the performance of the recommended models on a large and diverse dataset.

The linear filter is employed with coefficient W_K on the evaluated signal. The input signal, $x\left(n\right)$ comprise of noise, $v\left(n\right)$,

$$x\left(\mathrm{n}\right) = d\left(n\right) + v\left(n\right) \tag{1}$$

The output signal $y\left(n\right)$ needs to be a closer estimation of $d\left(n\right)$. Hence, the error signal $e\left(n\right)$ needs to be minimal. The adoptive method attempts to correct the weight W_K, thus the mean square error is minimized.

$$e = \min\left\{E\left[e\left(n\right)^2\right]\right\} \tag{2}$$

Whereas

$$e\left(n\right)=\mathrm{y}\left(\mathrm{n}\right)-d\left(n\right) \tag{3}$$

A k tap discrete WF employs the subsequent formula for finding the value of y (n)

$$y\left(n\right)=\sum_{k=0}^{N-1}W_{k}\left(d\left(n-k\right)*v\left(n-k\right)\right) \tag{4}$$

The Wiener-Hopf equation, estimates the optimum weight, is the primary feature of WF.

$$E_{l=0}^{p-\iota}W_{ol}r_{xx}\left(k-1\right)=r_{xd}\left(-l\right) \tag{5}$$

In which $W_{00},W_{01},\cdots\cdots\cdots,W_{op-1}$ indicates the optimal value of tap weight of the filter r_{xd} represent the cross-correlation function among $x\left(n\right)$ and $d\left(n\right)$, and r_{xx} indicates the auto-correlation operation of x(n).

2.2 EfficientNet based Feature Extraction

A recently created DL model with 53,26,716 parameters is called the EfficientNetMobile model. It demonstrates high dependability. A group of blocks are combined to form a cell, which is the basic building block of the EfficientNet model. The factorization of networks into cells and subsequent division into blocks creates the EfficientNet's search space. Cell/block sizes and types are not predetermined. They must, however, be tailored to the selected dataset. Convolution, separable convolution, maximum pooling, average pooling, and identify map make up the block's likely mode of operation. To extract an effective set of topographies, the EfficientNet prototypical is applied to derive feature vectors. EfficientNet is a convolutional neural network architecture and scaling method that uses a compound coefficient to uniformly scale all depth/width/resolution dimensions. Unlike traditional practise, which arbitrarily scales these factors, the EfficientNet scaling method uniformly scales network width, depth, and resolution using a fixed set of scaling coefficients. For example, if we want to use 2N times more computational resources, then we can simply increase the network depth by αN, width by βN, and image size by γN, where α,β,γ are constant coefficients determined by a small grid search on the original small model. EfficientNet uses a compound coefficient ϕ to uniformly scales network width, depth, and resolution in a principled way.The EfficientNet family is depending on a novel methodology to scale up the CNN model. It employs an effective compound coefficient. EfficientNet scales every dimension of the network using a fixed set of scaling coefficients, as opposed to the traditional approaches that scale the width, resolution, and depth of the network (Atila, Ü., 2021). A model's performance can be improved by scaling individual dimensions, but it can be improved much more by ensuring that all network dimensions make optimal use of available resources. EfficientNet is far more compact than other models while maintaining the same degree of accuracy on ImageNet. For comparison's sake, the ResNet50 architecture shown in the Keras application has 23,534,592 parameters, whereas the simplest EfficientNet (named EffecientNet-B0) has 5,330,564 parameters.

In this study, an effective method was used that was built on top of the EfficientNet-B3 CNN framework. Then, they settled on one EfficientNet variant because it strikes a better balance between precision and computational demands. The similar concept we presented here might be employed for the effective variant. MBConv depends on the concept borrowed from the MobileNet model. In MobileNetV2, a better module with inverted residual structure is introduced. Non-linearities in narrow layers are removed this time. With MobileNetV2 as the backbone for feature extraction, state-of-the-art performance is also achieved for object detection and semantic segmentation. One

primary concept is utilising depth wise separable convolution that comprises pointwise and depth wise convolutional layers. Following that, concepts from MobileNet-V2 (a modified version of MobileNet) are borrowed, including 1) linear bottleneck and 2) inverted residual connection. Fig. 2 demonstrates the EfficientNet baseline network.

2.3 Deep Transfer Learning

Whenever an image is being classified, the DTL model is the one responsible for giving it the relevant class labels. The Deep Thought Layer (DTL) is a probabilistic generation model that consists of a stack of restricted Boltzmann machine (RBM) and backpropagation (BP) neural networks. The output layer, the n-th hidden layer, and the visible layer make up its components respectively. The input and visible layer is located at the very end of the model. During the learning process, the features are transported through a number of hidden layers before arriving at the visible layer. At long last, the output layer will have the appropriate class label applied to it. In addition, RBM features input and hidden layers, as well as linkages that go in both directions between the different layers.

2.4 Hyperparameter Optimization

Optimal EfficientNet model hyperparameters are selected using the DPO technique. Because ducks have such a unique skill set, the DPO algorithm (Kamalraj, R., 2021) presents a fresh approach based on their foraging performance. Hyperparameters are distinct from parameters, which are the internal coefficients or weights found by the learning algorithm for a model. In contrast to parameters, hyperparameters are set by the practitioner when the model is configured. It is common to use random or grid search strategies for different hyperparameter values because it is difficult to know what values to use for the hyperparameters of a given algorithm on a given dataset. The more algorithm hyperparameters that must be tuned, the slower the tuning process. As a result, it is preferable to search for or tune a subset of model hyperparameters. Not all model hyperparameters are created equal. Some hyperparameters have a disproportionate impact on the behaviour, and thus the performance, of a machine learning algorithm. To get a good result quickly as a machine learning practitioner. This method revealed two options for the user to mimic duck feeding:

Figure 2.
EfficientNet baseline network

2.4.1 The Neural Operator

The neural operator was considered for imitating the duck package's play of imprinting performance. The play of imprinting performance was truly the function of nerves. The faster DPA reaches its destination, the less reliant it is on neural operators. It can be slowly dependent on the next operator.

2.4.2 Food Operator

For simulating the effect of food on duck packs, the food operator was considered. If the duck's method of food is dependent upon the direction of food further and slowly reduces depending on the neural operator. In this section, the mathematical model of the proposed method is shown in detail. Here, we talk about the three main things that DPO does: I Where the ducks are after waiting in line (population initialization), (ii) Looking for food (exploration phase), and (iii) Foraging in groups (Exploitation phase). Noting that there are two rules you need to follow when looking for food for ducks. Rule 1: When looking for food, ducks that are good at searching are closer to the centre of the food source. This makes other ducks move closer to them, and the updated location is also affected by the ducks that are close by. Rule 2: When foraging, all the ducks move toward the food. The next position is determined by the ducks around them, the position of the food, or the leader duck.

Given that the DPA has two distinct iteration loops, the neural operator is employed more often.

During the D dimension searching space, N ducks were arbitrarily initialized with its position and velocity represented as $X_i = \left[x_{i1},\ldots\ldots,x_{iD}\right]$ and $V_i = \left[v_i,\ldots\ldots,v_{iD}\right]$, whereas $i = 1,\ldots\ldots N$. All the ducks upgrade their position X_i and speed V_i based on Eq. (1):

$$y_i^{I_n} = y_i^{I_n-1} \times e^{-R\times I_n} + rand \times \left(X_B - X_i^{I_n-1}\right).$$
$$X_i^{I_n} = X_i^{I_n-1} + V_i^{I_n} \tag{6}$$

X_i Whereas R refers the neural factor and is artificially fixed to number amongst $zero$ and one. I_n refers the existing amount of iterations. X_B stands for the global optimum places attained by relating the position of every duck afterward $I_n - 1$ iteration cycle. The previous iteration loop is terminated and the neural operator is terminated after the requisite number of iterations. It is transferred to food operator X I, who continues to work with it.

$$X_c^{I_n-1} = \frac{\sum_{i=1}^{N^{I_n-1}} X_i^{I_n-1} \cdot f\left(X_i^{I_n-1}\right)}{N^{I_n-1} \cdot \Sigma_{i=1}^{N^{I_n-1}} f\left(X_i^{I_n-1}\right)},$$
$$N^{I_n} = \frac{N^{I_n-1}}{2},$$
$$X_i^{I_n} = X_i^{I_n-1} + rand \times \left(X_c^{I_n-1} - X_i^{I_n-1}\right) \tag{7}$$

Whereas:

$$f\left(X_{\mathrm{i}}^{I_n-1}\right) = \begin{cases} \dfrac{1}{filness\left(X_i^{l_n-1}\right) + \varepsilon}, & aiming\,at\,the\,minimization\,problem \\ fiTness\left(X_i^{l_n-1}\right), & aiming\,at\,the\,maximization\,problem \end{cases} \tag{8}$$

Similar to how the meal operator stops functioning once the preceding iteration has completed the necessary number of times, this one too will eventually reach its end state. In each of the two cycles, two operators are busy at once. For this reason, the solution to the above two equations dictates that gradual, actual-condition-based changes be made to the weights of two operators and the iterative loop used to combine their respective functions.

The particular upgrade approach was demonstrated as:

$$N^{I_n} = N^{I_n-1} - H \tag{9}$$

$$V_i^{l_n} = V_i^{l_n-1} \times e^{-R\times l_n} + rand \times [\left(1 - log_{l_{n\max}}^{l_n}\right)\left(X_B - X_i^{l_n-1}\right)$$

$$+loq_{I_{n\max}}^{I_n} \times \left(X_c^{l_n-1} - X_i^{l_n-1}\right);$$

$$X_i^{I_n} = X_i^{I_n-1} + V_i^{I_n} \tag{10}$$

Whereas H refers the amount of ducks discarded from all iterations and $I_{n\max}$ represents the maximal amount to iteration. With the enhancement of I_n, the effect of X_B on $X_i^{I_n}$ reduces and $X_i^{I_n}$ depends on $X_c^{I_n-1}$. As the design integrates the work of 2 operators from iterative loop and is slowly alteration the weighted of 2 operators based on the actual condition, for an optimum realizing the imitation of procedure of duck feeding.

There exists a marvel of engraving in the gathering of ducks. When ducks scavenge for food as a group, marking behaviour also plays an important role. When the ducks are farther away from food, the miracle of engraving causes the entire population to move in a fixed pattern. When the ducks are close to food, the entire flock is food-positioned, and they can finally get to where the food is effectively. The foraging behaviour of ducks can be divided into two categories. The preceding one is located by the marvel of engraving, and the final one is located by the food they finally discover in equation (11).

$$Osmotic\ Energy\ Calculation\ For\ Duck\ Flock \tag{11}$$
$$\pi = MRT$$

M is the molar concentration of dissolved species (units of mol/l). r is the ideal gas constant (0.08206 l atm mol-1 k -1, or other values depending on the pressure units). T is the temperature on the kelvin scale. Specialists and researchers are continually searching for better approaches to really focus on individuals with disease. To do this, they make and study new medications. They additionally search for better approaches to utilize drugs that are now accessible.

There are 3 fundamental strides in finding and building up another medication:

- preclinical examination, which is the point at which the medication is found and first, tried.
- clinical exploration, which is the point at which the medication is tried in individuals.
- post-clinical examination, which happens after the medication is endorsed

2.5 VAE Based Classification

After collecting the feature vectors, the VAE model is utilised to categorise the data (Kavitha, T., 2022). The topmost layer of the visual approach in VAE is the latent parameter z at which the generating mechanism begins. The complex process of data generation that results in the data x, is denoted as $g\left(z\right)$ viz modelled in the formation of ANN. The marginal probability can be attained by adding the

marginal probability of data point in (11). Eq (12) is attained when the marginal probability of data point is formulated by:

$$logp_{\theta}\left(x^{(1)},\ldots,x^{(N)}\right)=\sum_{i=1}^{N}logp_{\theta}\left(x^{(i)}\right) \tag{12}$$

$$logp_{\theta}\left(x^{(i)}\right)\geq\mathcal{L}\left(\theta,\varphi;x^{(i)}\right) \tag{12}$$

$$=E_{q_{\varphi}(z|x^{(i)})}\left[-logq_{\varphi}\left(z|x\right)+logp_{\theta}\left(x|z\right)\right] \tag{13}$$

$$=-D_{KL}(q_{\varphi}(z\mid x^{(i)})\,||\,p_{\theta}\left(z\right))+E_{q_{\varphi}(z|x^{(i)}}\left[logp_{\theta}\left(x|z\right)\right] \tag{14}$$

Where D_{KL} denotes the KullbackLeibler divergence between the posterior and previous estimates of the latent parameter z. Given the input dataset x, $p_{\theta}(x\mid z)$ represents the probability that the latent parameter z will be present. $q_{\varphi}\left(Zx\right)$, $p_{\theta}\left(xz\right)$

A neural network can estimate the posterior $q_{\varphi}\left(Zx\right)$, parameter using VAE. Encoder and decoder are represented by the directed probabilistic graphical model $p_{\theta}\left(xz\right)$ and the approximate posterior $q_{\varphi}\left(Zx\right)$. In this regard, it is essential to recall that the purpose of VAE modelling is the distribution parameter, not the true value. $p_{\theta}\left(xz\right)$ has a varied probability distribution based on the data type. A multivariate Gaussian distribution is utilised when the input dataset is continuous. For VAE training, the backpropagation approach is one possibility. The following term in (14) is computed using the Monte Carlo gradient method and a reparameterization technique that use a random parameter from a normal distribution instead of a random parameter from the original distribution. It may also be stated as follows:

$$Z=h_{\varphi}\left(,x\right)with\varepsilon\sim\mathcal{N}\left(0,1\right) \tag{15}$$

The reparameterization process assurance that Z follows the distribution of $q_{\varphi}(z\mid x)$.

3. EXPERIMENTAL VALIDATION

Biomarkers are components of cells found in body fluids or tumour cells that are overexpressed during the disease's onset. Cancer progresses through three major stages: initiation, promotion, and progression. All three steps are associated with significant changes in a cell's metabolome, transcriptome, and proteome. These modifications are the result of changes in particularly important genes or proteins, which result in the diversification or halting of critical metabolic and structural pathways. Using a benchmark dataset [19] containing 290 benign and 934 malignant pictures from 230 individuals, the DPODTL-OSCC model's performance is validated. A dataset with two categories, normal oral epithelium (NEOR) and squamous cell carcinoma of the oral cavity (OSCC), was used. To realise artificial intelligence of medial things, four deep learning (DL) models (VGG16, AlexNet, ResNet50, and Inception V3) were used to extract features from this dataset (AIoMT). Our experiment was showed applying an Intel Core i5 processor and 8 GB of RAM. Additionally, we utilized Jupiter Notebook with Python 3 Python's plethora of built-in packages, including NumPy, Pandas, SciPy, Matplotlib, and Standard Scale, is the primary reason for its adoption in the construction of diverse machine algorithms. Pictures are displayed as examples in Figure 3. It illustrates a number of confusion matrices that were produced by the DPODTL-OSCC model using a number of different TR/TS datasets. On a training/testing (TR/TS) set of 90: 10, the IDL-OSCDC model identified 9

samples as having cancer and 4 samples as having no evidence of cancer. The TR/TS set of 80:20 was followed by the DPODTL-OSCC approach, which resulted in 18 samples being categorised as cancer and 7 samples being classed as noncancer. In the meantime, the DPODTL-OSCC technique diagnosed 24 samples as cancer while classifying 14 samples as noncancer. This was done on the 70:30 TR/TS set. In conclusion, the DPODTL-OSCC system identified cancer in 28 of the samples on the TR/TS set of 60:40, while identifying noncancer in 22 of the samples.

This paper introduces EfficientNetV2, a new family of convolutional networks that can be trained faster and use their parameters more efficiently than older models. To make these models, we use a mix of training-aware neural architecture search and scaling to improve both the speed of training and the efficiency of the parameters. With progressive learning, our EfficientNetV2 does much better on the ImageNet and CIFAR/Cars/Flowers datasets than previous models. By pretraining on the same ImageNet21k, our EfficientNetV2 gets 97.31% top-1 accuracy on ImageNet ILSVRC2012. This is better than the recent ViT by 2.0% accuracy while training 5x–11x faster using the same computing resources.

Figure 4 shows the DPODTL-OSC3 model's output of two confusion matrices. With 70% of the training set (TRS), the DPODTL-OSC3 model has identified 638 samples of cancer and 195 samples of non-cancer images. Also, on 30% of the testing sets (TSS), the DPODTL-OSC3 approach has identified 269 samples of cancer and 89 samples of non-cancer images.

Table 2 displays the complete OSCC classification results for the DPODTL-OSC3 model based on 70 percent of the training data and 30 percent of the testing data. Figure 5 illustrates a rapid evaluation of the DPODTL-OSC3 model utilising 70% of the training data.The DPODTL-OSC3 model has classified the images into cancer class with $accu_y$, $prec_n$, $reca_l$, $spec_y$, and F_{score} of 97.31%, 99.38%, 97.11%, 97.99%, and 98.23% respectively. In addition, the DPODTL-OSC3 model has recognized the images into non-cancer class with $accu_y$, $prec_n$, $reca_l$, $spec_y$, and F_{score} of

Figure 3.
Sample images

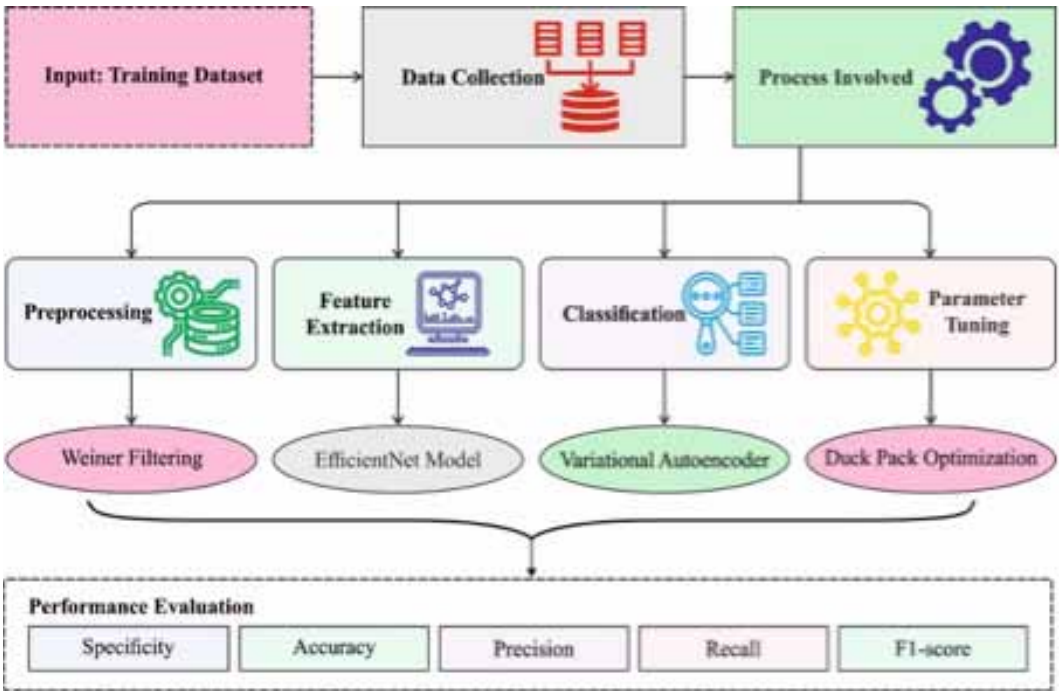

Figure 4.
Confusion matrix of DPODTL-OSC3 technique

Stage	Operator	Resolution	#Channels	#Layers
1	Conv3x3	224 x 224	32	1
2	MBConv1, k3x3	112 x 112	16	1
3	MBConv6, k3x3	112 x 112	24	2
4	MBConv6, k5x5	56 x 56	40	2
5	MBConv6, k3x3	28 x 28	80	3
6	MBConv6, k5x5	14 x 14	112	3
7	MBConv6, k5x5	14 x 14	192	4
8	MBConv6, k3x3	7 x 7	320	1
9	Conv1x1 and Pooling and FC	7 x 7	1280	1

Table 2.
DPODTL-OSC3 technique result analysis with unique measures

Class Labels	Accuracy	Precision	Recall	Specificity	F-Score
Training Samples (70%)					
Cancer	97.31	99.38	97.11	97.99	98.23
Non-Cancer	97.31	91.12	97.99	97.11	94.43
Average	**97.31**	**95.25**	**97.55**	**97.55**	**96.33**
Testing Samples (30%)					
Cancer	97.28	99.26	97.11	97.80	98.18
Non-Cancer	97.28	91.75	97.80	97.11	94.68
Average	**97.28**	**95.51**	**97.46**	**97.46**	**96.43**

97.31%, 91.12%, 97.99%, 97.11%, and 94.43% respectively. Besides, the DPODTL-OSC3 model has classified the images with average $accu_y$, $prec_n$, $reca_l$, $spec_y$, and F_{score} of 97.31%, 95.25%, 97.55%, 97.55%, and 96.33% respectively.

Figure 6 demonstrates a brief result analysis of the DPODTL-OSC3 method with 30% of testing data. The DPODTL-OSC3 model has classified the images into cancer class with $accu_y$, $prec_n$, $reca_l$, $spec_y$, and F_{score} of 97.28%, 99.26%, 97.11%, 97.80%, and 98.18% correspondingly. Besides, the DPODTL-OSC3 approach has recognized the images into non-cancer class with $accu_y$, $prec_n$,

Figure 5.
DPODTL-OSC3 method result analysis on 70% of TRS data

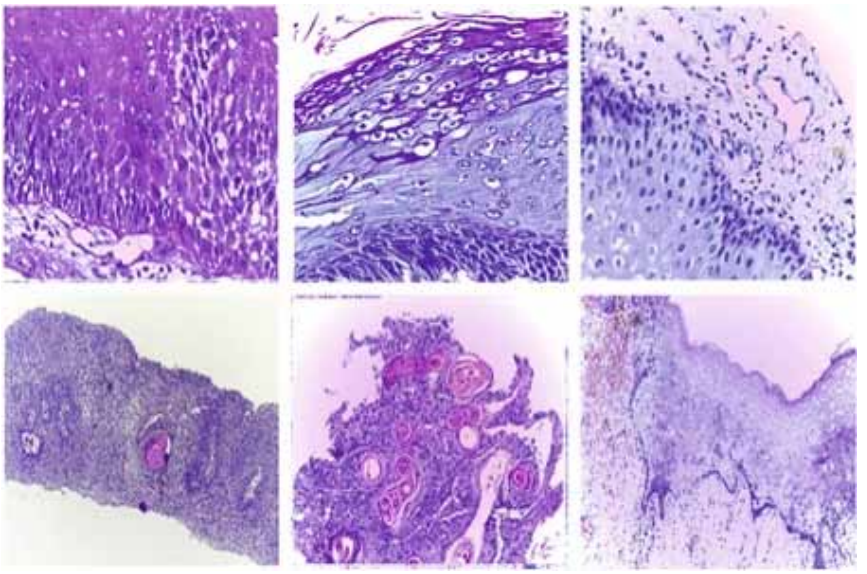

Figure 6.
DPODTL-OSC3 method result analysis on 30% of TSS data

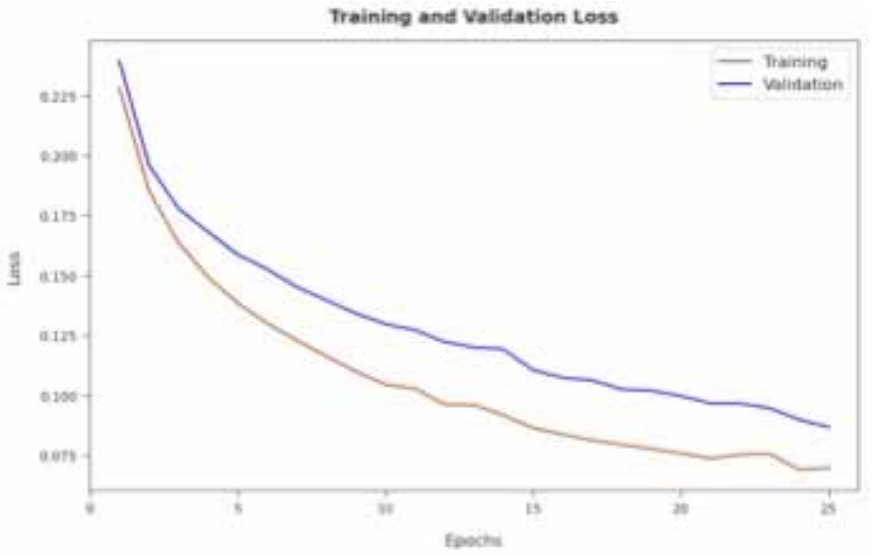

$reca_l$, $spec_y$, and F_{score} of 97.28%, 91.75%, 97.80%, 97.11%, and 94.68% correspondingly. In addition, the DPODTL-OSC3 technique has classified the images with average $accu_y$, $prec_n$, $reca_l$, $spec_y$, and F_{score} of 97.28%, 95.51%, 97.46%, 97.46%, and 96.43% respectively.

Figure 7 depicts the validation and training accurateness of the DPODTL-OSC3 prototypical on the test dataset. According to the findings of the studies, the TA and VA values of the DPODTL-OSC3

Figure 7.
TA and VA graph analysis of DPODTL-OSC3 technique

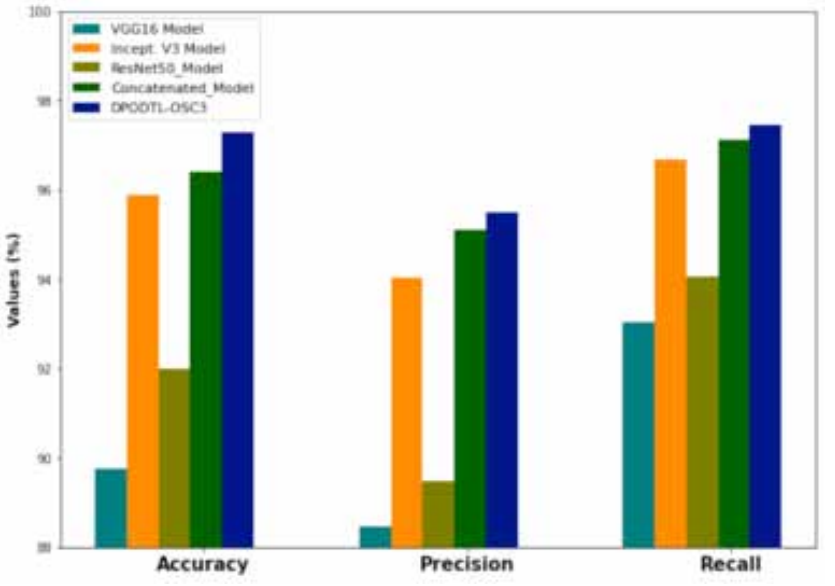

model have reached their maximum levels. In particular, VA appears to be superior over TA. The DPODTL-OSC3 model's training loss (TL) and validation loss (VL) on the test dataset are shown in Figure 8.The DPODTL-OSC3 model was estimated to have the least TL and VL values based on experimental results. It appeared that the VL was shorter than the TL.

$spec_y$ and F_{score} In Table 3, we see the results of classifying the DPODTL-OSC3 model against other models on a variety of metrics. Figure 8 compares the extensive specifications and F score of the DPODTL-OSC3 approach to earlier models. The ResNet50 and VGG16 models had lower s $spec_y$ and F_{score} values, according to the data. Followed by, the Inception v3 and Concatenated model has shown slightly enhanced values of $spec_y$ and F_{score}. However, the DPODTL-OSC3 model has outperformed the other methods by accomplishing maximum $spec_y$ and F_{score} values of 97.46% and 96.43% respectively.

Figure 9 and Figure.10 examines a detailed acc_y, $prec_n$, and $reca_l$ and RSME of the DPODTL-OSC3 technique with fresh replicas. The results referred that the ResNet50 and VGG16 replicas have obtained lesser standards of acc_y, $prec_n$, and $reca_l$. Likewise, the Inception v3 and Concatenated

Table 3.
DPODTL-OSC3 methodology compared to existing methods

Methods	Accuracy	Precision	Recall	Specificity	F1-score
VGG16 Model	89.75	88.47	93.04	88.17	90.69
Incept. V3 Model	95.88	94.05	96.70	94.42	95.32
ResNet50 Model	92.00	89.48	94.07	88.90	92.09
Concatenated Model	96.40	95.11	97.13	96.29	95.72
DPODTL-OSC3	97.28	95.51	97.46	97.46	96.43

Figure 8.
$Spec_f$ **and** $F1_{score}$ **analysis of DPODTL-OSC3 technique with existing methods**

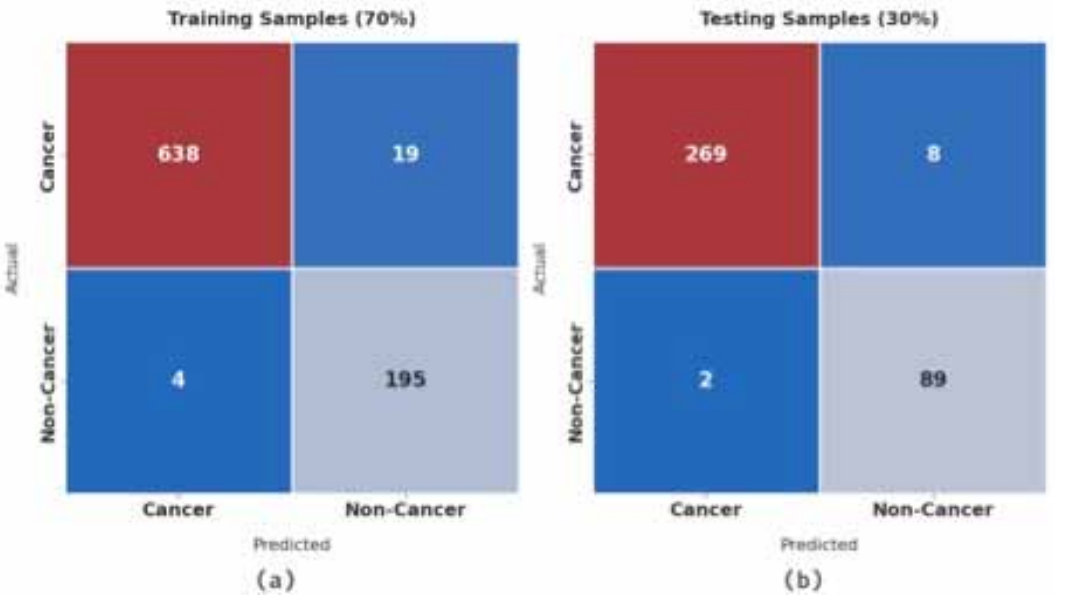

Figure 9.
Comparison of the DPODTL-OSC3 method to existing techniques

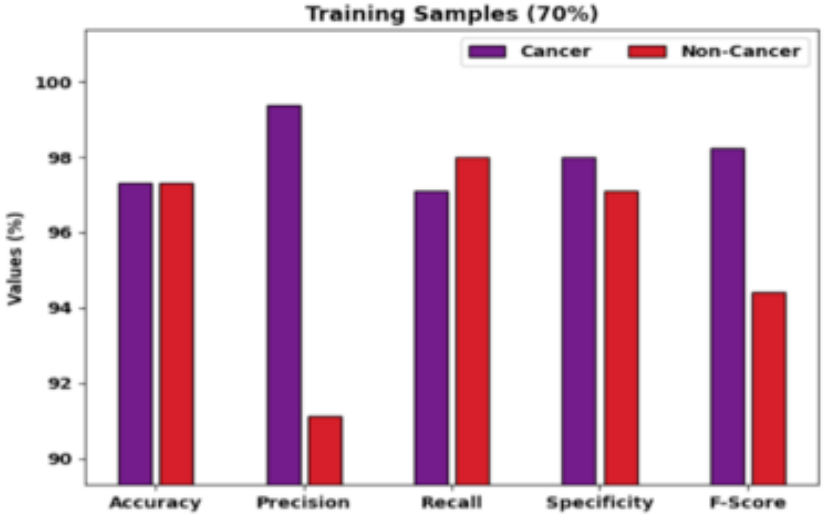

technique has shown slightly enhanced values of acc_y, $prec_n$, and $reca_l$. But, the DPODTL-OSC3 approach has outperformed the other methods by accomplishing maximum acc_y, $prec_n$, and $reca_l$ values of 97.28%, 95.51%, and 97.46% correspondingly. After inspecting the consequences and conversation in detail, it is confirmed that the DPODTL-OSC3 model has effectively classified the

Figure 10.
RSME Comparison of the DPODTL-OSC3 method to existing techniques

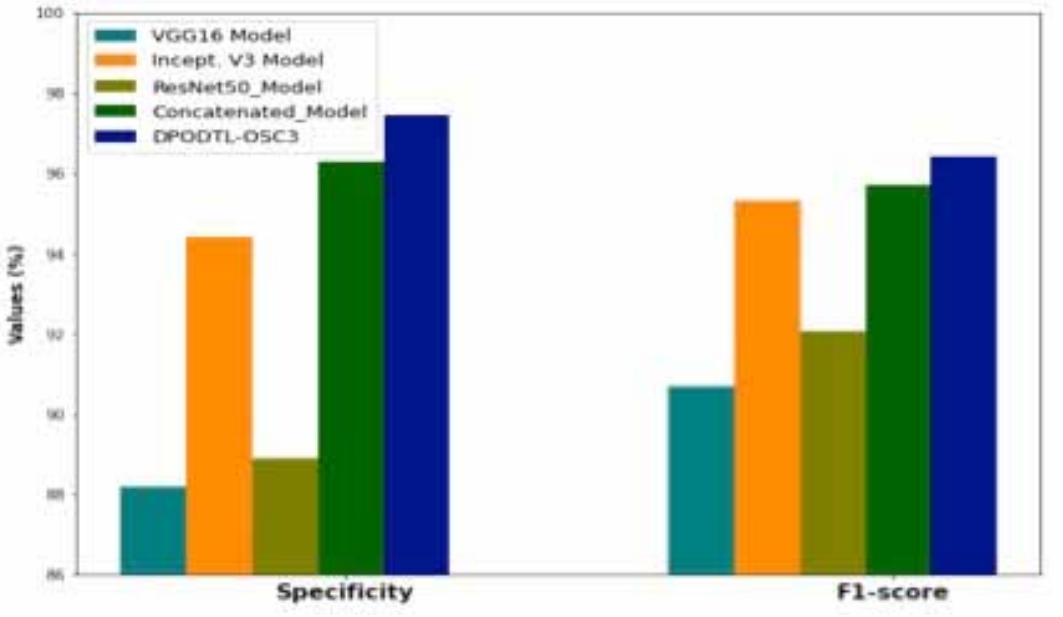

histopathological images. DPODTL-OSC3 prototypical has claimed lowest error rate for all the range of data rather than existing methods.

4. CONCLUSION

In this study, new DPODTL-OSC3 models for OSCC.WF-based pre-processing classification were created. EfficientNet, a DPO-based hyperparameter optimizer, and VAE-based cataloguing are the three components that make up the DPODTL-OSC3 model that was suggested. The DPO algorithm's structure lends a hand in determining the best values to set its hyperparameters to. The effectiveness of the DPODTL-OSC3 model is evaluated by means of an experimental validation procedure applied to the histopathology imaging database. In a comparison outcome analysis, the DPODTL-OSC3 model fared better than the competing methods. As a result, OSCCs can be precisely classified using the DPODTL-OSCC model. In the not too distant future, researchers will be able to enhance the framework for both transfer learning and machine learning by making use of real-time data and a vast database. This discovery can also be applied to the histopathology-based staging of oral squamous cancer. The ability to treat patients more successfully will allow doctors to potentially save more lives.

REFERENCES

Ahmed, U., Issa, G. F., Khan, M. A., Aftab, S., Said, R. A. T., Ghazal, T. M., & Ahmad, M. (2022). Prediction of Diabetes Empowered with Fused Machine Learning. *IEEE Access: Practical Innovations, Open Solutions*, *10*, 8529–8538. doi:10.1109/ACCESS.2022.3142097

Alabi, R. O., Youssef, O., Pirinen, M., Elmusrati, M., Mäkitie, A. A., Leivo, I., & Almangush, A. (2021). A Machine learning in oral squamous cell carcinoma: Status, clinical concerns and prospects for future—A systematic review. *Artificial Intelligence in Medicine*, *115*, 102060. doi:10.1016/j.artmed.2021.102060 PMID:34001326

Alkhadar, H., Macluskey, M., White, S., Ellis, I., & Gardner, A. (2021). Comparison of machine learning algorithms for the prediction of five-year survival in oral squamous cell carcinoma. *Journal of Oral Pathology & Medicine*, *50*(4), 378–384. doi:10.1111/jop.13135 PMID:33220109

AminI.ZamirH.KhanF. F. (2021). Histopathological Image Analysis for Oral Squamous Cell Carcinoma classification using concatenated deep learning models. medRxiv. 10.1101/2021.05.06.21256741

Arun, A., Bhukya, R. R., Hardas, B. M., Kumar, T., & Ashok, M. (2022). An automated word embedding with parameter tuned model for web crawling. *Intelligent Automation & Soft Computing*, *32*(3), 1617–1632. doi:10.32604/iasc.2022.022209

Atila, Ü., Uçar, M., Akyol, K., & Uçar, E. (2021). Plant leaf disease classification using EfficientNet deep learning model. *Ecological Informatics*, *61*, 101182. doi:10.1016/j.ecoinf.2020.101182

Chu, C. S., Lee, N. P., Ho, J. W., Choi, S. W., & Thomson, P. J. (2021). Deep learning for clinical image analyses in oral squamous cell carcinoma: A review. *JAMA Otolaryngology-Head & Neck Surgery*, *147*(10), 893–900. doi:10.1001/jamaoto.2021.2028 PMID:34410314

Cyril, C. P. D., Beulah, J. R., Subramani, N., Mohan, P., Harshavardhan, A., & Sivabalaselvamani, D. (2021). An automated learning model for sentiment analysis and data classification of Twitter data using balanced CA-SVM. *Concurrent Engineering*, *29*(4), 386–395. doi:10.1177/1063293X211031485

Das, D. K., Bose, S., Maiti, A. K., Mitra, B., Mukherjee, G., & Dutta, P. K. (2018). Automatic identification of clinically relevant regions from oral tissue histological images for oral squamous cell carcinoma diagnosis. *Tissue & Cell*, *53*, 111–119. doi:10.1016/j.tice.2018.06.004 PMID:30060821

Fraz, M. M., Khurram, S. A., Graham, S., Shaban, M., Hassan, M., Loya, A., & Rajpoot, N. M. (2020). FABnet: Feature attention-based network for simultaneous segmentation of microvessels and nerves in routine histology images of oral cancer. *Neural Computing & Applications*, *32*(14), 9915–9928. doi:10.1007/s00521-019-04516-y

Hardas, B. M., & Pokle, S. B. (2017). Optimization of Peak to Average Power Reduction in OFDM. *Journal of Communications Technology and Electronics*, *62*(12), 1388–1395. doi:10.1134/S1064226917140017

Jain, M., Kasetty, S., Sudheendra, U. S., Tijare, M., Khan, S., & Desai, A. (2014). Assessment of tissue eosinophilia as a prognosticator in oral epithelial dysplasia and oral squamous cell carcinoma—An image analysis study. *Pathology Research International*, *2014*, 2014. doi:10.1155/2014/507512 PMID:24693457

Jaishankar, B., Vishwakarma, S., Aditya Kumar, S. P., Ibrahim, P., & Arulkumar, N. (2022). Blockchain for Securing Healthcare Data Using Squirrel Search Optimization Algorithm. *Intell. Autom. Soft Comput*, *32*(3), 1815–1829. doi:10.32604/iasc.2022.021822

Kamalraj, R., Neelakandan, S., Kumar, M. R., Rao, V. C. S., Anand, R., & Singh, H. (2021). Interpretable filter based convolutional neural network (IF-CNN) for glucose prediction and classification using PD-SS algorithm. *Measurement*, *183*, 109804. doi:10.1016/j.measurement.2021.109804

Kavitha, T., Mathai, P. P., Karthikeyan, C., Ashok, M., Kohar, R., Avanija, J., & Neelakandan, S. (2022). Deep learning based capsule neural network model for breast cancer diagnosis using mammogram images. *Interdisciplinary Sciences, Computational Life Sciences*, *14*(1), 113–129. doi:10.1007/s12539-021-00467-y PMID:34338956

Kikuta, S., Iwanaga, J., Todoroki, K., Shinozaki, K., Tanoue, R., Nakamura, M., & Kusukawa, J. (2018). Clinical Application of the IllumiScan Fluorescence Visualization Device in Detecting Oral Mucosal Lesions. *Cureus*, *6*, e3111. doi:10.7759/cureus.3111 PMID:30338186

Kozakai, A., Ono, K., Nomura, T., Takano, T., & Shibahara, T. (2020). Usefulness of objective evaluations by fluorescence visualization device for differentiating between superficial oral squamous cell carcinoma and oral lichen planus. *Journal of Oral and Maxillofacial Surgery, Medicine, and Pathology*, *32*(1), 26–32. doi:10.1016/j.ajoms.2019.09.010

Manju, B. R., & Sneha, M. R. (2020). ECG denoising using wiener filter and kalman filter. *Procedia Computer Science*, *171*, 273–281. doi:10.1016/j.procs.2020.04.029

Mishra, S., & Prakash, M. (2022). Digital Mammogram Inferencing System Using Intuitionistic Fuzzy Theory. *Computer Systems Science and Engineering*, *41*(3), 1099–1115. doi:10.32604/csse.2022.020439

Musulin, J., Štifanić, D., Zulijani, A., Ćabov, T., Dekanić, A., & Car, Z. (2021). An enhanced histopathology analysis: An ai-based system for multiclass grading of oral squamous cell carcinoma and segmenting of epithelial and stromal tissue. *Cancers (Basel)*, *13*(8), 1784. doi:10.3390/cancers13081784 PMID:33917952

Panigrahi, S., Das, J., & Swarnkar, T. (2020). Capsule network based analysis of histopathological images of oral squamous cell carcinoma. *Journal of King Saud University-Computer and Information Sciences*.

Panigrahi, S., & Swarnkar, T. (2020). Machine learning techniques used for the histopathological image analysis of oral cancer-a review. *The Open Bioinformatics Journal*, *13*(1), 106–118. doi:10.2174/1875036202013010106

Pokle, S. B. (2019). Analysis of OFDM system using DCT-PTS-SLM based approach for multimedia applications. *Cluster Computing*, *22*(2), 4561–4569.

Rahman, T. Y., Mahanta, L. B., Das, A. K., & Sarma, J. D. (2020). Automated oral squamous cell carcinoma identification using shape, texture and color features of whole image strips. *Tissue & Cell*, *63*, 101322. doi:10.1016/j.tice.2019.101322 PMID:32223950

Rahman, T. Y., Mahanta, L. B., Das, A. K., & Sarma, J. D. (2020). Histopathological imaging database for oral cancer analysis. *Data in Brief*, *29*, 105114. doi:10.1016/j.dib.2020.105114 PMID:32021884

Rahman, T. Y., Mahanta, L. B., Chakraborty, C., Das, A. K., & Sarma, J. D. (2018). Textural pattern classification for oral squamous cell carcinoma. *Journal of Microscopy*, *269*(1), 85–93. doi:10.1111/jmi.12611 PMID:28768053

Reshma, G., Al-Atroshi, C., Nassa, V. K., Geetha, B., Sunitha, G., & Galety, M. G. (2022). Deep learning-based skin lesion diagnosis model using dermoscopic images. *Intell. Autom. Soft Comput*, *31*(1), 621–634. doi:10.32604/iasc.2022.019117

Saravanakumar, C., Priscilla, R., Prabha, B., Kavitha, A., Prakash, M., & Arun, C. (2022). An Efficient On-Demand Virtual Machine Migration in Cloud Using Common Deployment Model. *Computer Systems Science and Engineering*, *42*(1), 245–256. doi:10.32604/csse.2022.022122

Sultan, A. S., Elgharib, M. A., Tavares, T., Jessri, M., & Basile, J. R. (2020). The use of artificial intelligence, machine learning and deep learning in oncologic histopathology. *Journal of Oral Pathology & Medicine*, *49*(9), 849–856. doi:10.1111/jop.13042 PMID:32449232

Sunitha, G., Geetha, K., Neelakandan, S., Pundir, A. K. S., Hemalatha, S., & Kumar, V. (2022). Intelligent deep learning based ethnicity recognition and classification using facial images. *Image and Vision Computing*, *121*, 104404. doi:10.1016/j.imavis.2022.104404

Wang, W., Wu, S., & Lu, K. (2017, May). Duck pack algorithm—A new swarm intelligence algorithm for route planning based on imprinting behavior. In *2017 29th Chinese Control And Decision Conference (CCDC)* (pp. 2392-2396). IEEE.

Zavrak, S., & İskefiyeli, M. (2020). Anomaly-based intrusion detection from network flow features using variational autoencoder. *IEEE Access: Practical Innovations, Open Solutions*, *8*, 108346–108358. doi:10.1109/ACCESS.2020.3001350

Romano, A., Di Stasio, D., Petruzzi, M., Fiori, F., Lajolo, C., Santarelli, A., Lucchese, A., Serpico, R., & Contaldo, M. (2021, June 8). Noninvasive Imaging Methods to Improve the Diagnosis of Oral Carcinoma and Its Precursors: State of the Art and Proposal of a Three-Step Diagnostic Process. *Cancers (Basel)*, *13*(12), 2864. doi:10.3390/cancers13122864 PMID:34201237

Luz, E., Silva, P., Silva, R., Silva, L., Guimarães, J., Miozzo, G., Moreira, G., & Menotti, D. (2021). Towards an effective and efficient deep learning model for COVID-19 patterns detection in X-ray images. *Research on Biomedical Engineering*, 1–14.

Savita K Shetty is an M.Tech degree holder and is currently working as an assistant professor in the Information Science & Engineering Department of Ramaiah Institute of Technology. She is interested in subjects related to Data Mining and Data Analytics.

Dr Annapurna P. Patil is working as a Professor and Head in the Department of Computer Science & Engineering, Ramaiah Institute of Technology. Her areas of interest include Cloud Computing, Artificial Intelligence, Protocol Engineering, Wireless Networks, Data Structures, and Analysis of Algorithms, Machine learning and Data Analytics.